Volume 1, Number 1 (December 2005) p. 15-34 ISSN 1809-5046
Revista IBRACON de Materiais
IBRACON Materials Journal

Microstructural Analysis of Carbonated Concretes Containing Mineral Admixtures

Análise Microestrutural de Concretos Carbonatados Contendo Adições Minerais

A. DE CASTRO [A]
A. N. M. LOPES [B]
N. P. HASPARYK [C]
H. CARASEK [D]
O. CASCUDO [e]

Abstract

The aim of the study is to investigate the microstructural changes resulting from the use of mineral admixtures in portland cement as well as to assess the effect of carbonation on the hydration products formed.

Six different types of concrete were developed, constituted by binary mixtures of portland cement, each with the following contents (in partial replacement of cement) and admixtures types: silica fume 10 %, metakaolin 10 %, rice-husk ash 10 %, fly-ash 25 %, blast-furnace slag 65 % and normal portland cement (no-admixtures). After a period of 28 days in the moist room, followed by a complementary period of approximately 100 days in laboratory environment, the concretes underwent a CO_2 attack (5 % content) for two weeks and samples of these concretes were analyzed by means of scanning electron microscopy (SEM) and X-ray diffractometry (XRD).

As main results, it was verified that: among the concretes, those produced with rice-husk ash and silica fume yielded the highest relative compactness; in the morphology study, it was noted that in addition to the occurrence of calcite (main carbonation product), there was C-S-H carbonation and the formation of C-A-S-H, the latter resulting from the employment of admixtures with a high alumina content (as metakaolin, fly-ash and blast-furnace slag, for example). In the XRD analysis, the significant occurrence of the compound calcite was verified, which was not verified in some SEM analyses, which did not always clearly reveal that compound.

Keywords: carbonation; concrete; durability; microstructure; mineral admixture; scanning electron microscopy; X-ray diffraction.

Resumo

O objetivo deste trabalho é estudar as alterações microestruturais decorrentes da utilização de adições minerais em concretos de cimento Portland, assim como avaliar o efeito da carbonatação sobre os produtos de hidratação formados. Foram desenvolvidos seis diferentes concretos, constituídos por misturas binárias de cimento Portland CP II F com cada um dos seguintes teores (em substituição parcial ao cimento, em massa) e tipos de adição: 10% de sílica ativa, 10% de metacaulim, 10% de cinza de casca de arroz, 25% de cinza volante, 65% de escória de alto-forno e referência (sem adição). Após um período de 28 dias em câmara úmida, seguido de um período complementar de aproximadamente 100 dias em ambiente de laboratório, os concretos foram submetidos ao ataque de CO_2 (teor de 5%) por duas semanas e amostras desses concretos foram analisadas empregando-se as técnicas de microscopia eletrônica de varredura (MEV) e difratometria de raios X (DRX). Como resultados principais verificou-se que: dentre todos os concretos, os produzidos com cinza de casca de arroz e sílica ativa apresentaram as maiores compacidades relativas; no estudo da morfologia, observou-se que além da ocorrência de calcita (principal produto da carbonatação) também foi verificada a carbonatação do C-S-H e a formação de C-A-S-H, produto este decorrente do emprego de adições que possuem alto teor de alumina (como, por exemplo, metacaulim, cinza volante e escória de alto-forno). Na análise por DRX, verificou-se uma ocorrência significativa do composto calcita, o que não foi verificado em algumas análises por MEV, que por vezes não evidenciavam de forma clara tal composto.

Palavras-chave: adição mineral, carbonatação, concreto, difração de raios-X, durabilidade, microestrutura, microscopia eletrônica de varredura.

[a] Civil Engineer, he obtained a Master´s degree in Civil Engineering in the field of concrete durability in 2003 from the Federal University of Goiás, Brazil. He works at Department of Support and Technical Control of FURNAS Centrais Elétricas S. A. Currently, he develops research in the field of concrete technology and durability analysis in reinforced concrete.

[b] PhD candidate, works at the Civil Engineering Center at the Departament of Technical Support and Control of FURNAS Centrais Elétricas S.A, Brazil. She received her Master's Degree by the University of Brasilia in 1999. Her research interests include durability and concrete technology.

[c] Civil Engineer and works at Department of Support and Technical Control of FURNAS Centrais Elétricas S. A. in Goiânia/GO-Brazil and received her Master's degree on alkali-aggregate reaction in Federal University of Goiás in 1999. She is PhD Candidate in Federal University of Rio Grande do Sul (Brazil) and her research interests include microstructure and durability of cement-based materials.

[d] Professor of Civil Engineering at Federal University of Goiás, in Brazil. She received her Master's degree from the Federal University of Rio Grande do Sul and her PhD degree from the University of São Paulo, both in Brazil. She also performed a Post-Doctorate in the Institut National des Sciences Appliquées – INSA, in Toulouse, France. Her research interests include durability of cement-based materials.

[e] Professor of Civil Engineering at Federal University of Goiás, in Brazil. He received his Master and PhD degree from the University of São Paulo, in Brazil, and performed a Post-Doctorate in the Institut National des Sciences Appliquées – INSA, in Toulouse, France. His research interests include durability of concrete structures and science-technology of materials.

© 2005 IBRACON

1 Introduction

The use of mineral admixtures has made important contributions to the performance of concrete structures in the following aspects: economical, with the energy reduction in the production of the binder; environmental, given the use of industrial byproducts; and technical, by improving the properties of concrete and, consequently, increasing its durability [1, 2]. Sabir et al.[3] go as far as to postulate that the most important step in concrete development in the last century was the introduction of these byproducts, including fly-ash, blast-furnace slag and silica fume, in the production of concrete. This practice has now been extended to other residues, such as rice-husk ash and metakaolin.

Mineral admixtures can react with cement hydration products, and the main chemical reaction, denominated pozzolanic reaction, is facilitated by the dissociation of amorphous silica (deriving from these additions), producing silica in the pore solution, which then reacts with calcium hydroxide to form C-S-H gel. The technical relevance of this pozzolanic reaction derives mainly from three aspects: it is generally a slow reaction and therefore the rates of heat release and strength development are slow; it is a reaction that consumes calcium hydroxide, which constitutes a major contribution to the durability of hardened cement paste against acid environments; and lastly, studies on pore size distribution in hydrated cement pastes have shown that the reaction products are quite effective in filling up voids, obstructing large capillary pores (filler effect), thus improving the strength and reducing the system's permeability [2-4].

In the specific case of concrete carbonation, the reduction in the amount of calcium hydroxide, resulting from the pozzolanic reactions, would accelerate the carbonation process, in this way increasing the risk of reinforcement corrosion. However, when this effect is analyzed in conjunction with microstructural alterations, it becomes extremely difficult to predict concrete behavior because the mineral admixtures afford it substantially lower permeability, affecting transport mechanisms, including water absorption and the diffusion of carbonic gas and oxygen – agents which are directly linked to depassivation and reinforcement corrosion.

This paper presents part of the results for an experimental study conducted at the Civil Engineering Technological Center of FURNAS (Goiânia, Brazil), and was the object of a Master Degree Dissertation [5] carried out at the Federal University of Goiás.

2 Concrete Carbonation

The carbonation of concrete involves several physiochemical processes, namely: gaseous CO_2 diffusion in the concrete pores; CO_2 dissolution in the pore water; dissolution and diffusion of calcium hydroxide in the pore water; and lastly, CO_2 reaction with calcium hydroxide, producing calcium carbonate [6].

However, the action of CO_2 on cement constituents is a complex one as it is not limited to calcium hydroxide, also attacking the calcium silicate hydrate (C-S-H) and calcium aluminate phases. Taylor[7] describes the carbonation of cement hydration products as leading to the production of silica and alumina gels, in addition to calcium carbonate. The C-S-H is initially decalcified, thus reducing its Ca/Si ratio, and is later converted into silica gel. The hydrated aluminates (C_4AH_x) are rapidly converted into $C_4A\overline{C}H_x$ and then into alumina gel, while ettringite and monosulfate produce alumina gel and gypsum.

Some papers on C-S-H decomposition due to carbonation confirm that reduction in the values of the Ca/Si ratio. Nishikawa and Suzuki[8] noted that, in portland cement pastes of a w/c equal to 0.45, the Ca/Si ratio of C-S-H which was initially equal to 2.0 declined to values close to 1.0 (after 365 days under attack with a 5% concentration of CO_2), also verified values below 1.0 for the Ca/Si ratio of C-S-H in several concrete structures with ages ranging from 10 to 70 years. Kobayashi et al.[9] compared concrete structures with blast-furnace slag of ages between 10 and 34 years and noted values for the Ca/Si ratio between 0.17 and 0.57, in the carbonated samples, and values between 1.0 and 1.43, for the non-carbonated samples.

Famy et al. [10], studied the changes in C-S-H shades under scanning electron microscopy in polished samples of carbonated concrete, verified the decomposition of C-S-H. According to these authors, the light regions seen around the alite grains comprised calcium carbonate, while the dark regions (noted internally in grains and almost in all smaller grains) comprised silica gels, which was characterized as an indication of the Ca/Si ratio of C-S-H. Matsushita et al [11] studied the calcium silicate structure and the mechanism of carbonation shrinkage, with ^{29}Si MAS NMR spectroscopy, and they observed that when the degree of carbonation (relationship between the amount of combined carbon dioxide in a sample and that when all calcium oxide transformed to calcium carbonated) increased from 25 % to 50 % or 60 %, the double-chain silicate anion structure of tobermorite-11 Å was decomposed and Ca ions in the Ca-O layer were dissolved.

In addition, the calcium carbonate (main compound resulting from carbonation) may occur as three polymorphs, namely calcite, aragonite and vaterite. Highway Research Board[12] affirms that the aragonite may transform to calcite over long time periods and that the vaterite is metastable and it is often formed along with calcite as carbonation products of calcium silicate and aluminate hydrates. Alcocel et al.[13], studying the carbonation of the calcium aluminate cement, observed that the formation of aragonite and vaterite depends on manufacturing temperature and treatment conditions and the prevailing polymorphic variety is calcite.

3 Experimental Program

3.1 Materials Employed

a) Fine aggregate: river-bed natural sand, classified as fine sand and met specifications by ABNT NBR 7211:1983[14]. As its main mineralogical constitution it features quartz and has as subordinated components feldspate, muscovite, biotite, chlorite, opaque minerals and iron hydroxide.

b) Coarse aggregate: crushed Mica-schist rock with maximum size aggregate equal 19 mm and met specifications by ABNT NBR 7211:1983 [14]. As its main mineralogical constitution it features quartz, biotite/muscovite, garnet and chlorite/opaques.

c) Portland cement: CP II F brazilian portland cement, in compliance with ABNT NBR 11578:1991 [15]. This type of cement features additions of carbonatic materials with contents between 6 % and 10 %. Their main characteristics are shown in Table 1.

d) Mineral admixtures: silica fume, blast-furnace slag, rice-husk ash, fly-ash and metakaolin, whose main characteristics are shown in Table 1.

Table 1 – Main characteristics of the binder.

Characteristic or Determined Property		CP II F Portland Cement	Silica Fume	Meta-kaolin	Rice-husk Ash	Blast-furnace slag	Fly-ash
Specific gravity (kg/dm³)		3.0	2.2	2.5	2.2	2.9	2.3
BET specific area (m²/kg)		(a)	15,990	21,250	19,690	900	1,500
Chemical Components (%)	Loss of ignition	6.6	4.1	4.3	9.8	0.3	1.2
	Silicon dioxide (SiO_2)	18.7	91.1	46.7	82.8	35.0	62.0
	Aluminium oxide (Al_2O_3)	5.1	0.2	41.4	0.5	12.4	23.3
	Iron oxide (Fe_2O_3)	3.3	0.3	3.5	2.0	0.2	5.4
	Total calcium oxide (CaO)	62.4	0.8	0.5	1.1	41.6	2.0
	Magnesium oxide (MgO)	0.7	0.8	0.5	1.3	8.7	1.9
	Sodium oxide (Na_2O)	0.3	0.2	0.0	0.2	0.3	0.4
	Potassium oxide (K_2O)	0.5	0.3	0.3	0.6	0.6	3.0
	Alkaline equivalent	0.7	0.4	0.2	0.6	0.7	2.4
	Sulfuric anhydride (SO_3)	3.1	0.5	0.6	0.1	0.1	-

(a) Blaine specific area of cement = 3,860 m²/kg.

3.2 Studied Concretes

The concretes had their materials proportioning defined in a mixture proportion study in which the method employed by the Technological Center of FURNAS Centrais Elétricas S.A. [16] was adopted, and which is based on the experimental development of several combinations among the aggregates (altering the fineness module of the mixture), so as to minimize cement content without loss of mechanical strength and concrete workability. Table 2 shows the characteristics of the concrete proportions.

Table 2 – Main characteristics of the binder.

Concrete	Admixture content (%) (a)	Water-cementitious materials ratio (w/cm)	Binder content (kg/m³)	Cement content (kg/m³)	Mass mixture of binder (cement : admixture : sand : crushed agg.)
Reference	0	0.70	274	274.0	1.00 : 0.00 : 2.61 : 4.28
Slag	65	0.70	274	95.9	0.35 : 0.65 : 2.60 : 4.28
Fly-ash	25	0.70	274	205.5	0.75 : 0.25 : 2.58 : 4.24
Rice-husk ash	10	0.70	274	246.6	0.90 : 0.10 : 2.60 : 4.26
Metakaolin	10	0.70	274	246.6	0.90 : 0.10 : 2.60 : 4.26
Silica Fume	10	0.70	274	246.6	0.90 : 0.10 : 2.60 : 4.26

Mortar content, in mass, 0.46. (a) Cement replacement content, in mass.

Prismatic test specimens were cast in the size 75 mm x 120 mm x 300 mm, as illustrated in Fig.1a. After undergoing a curing period of 28 days in a moist room (at a temperature of 21°C and relative humidity above 90 %) and a follow-up period of approximately 100 days in laboratory environment, sheltered from weather changes, these test specimens were submitted to the CO_2 attack in a chamber with climatic control at temperatures of (28±1)oC, relative humidity of 65 % and carbonic gas concentration between 5 % and 6 %.

3.3 Test Samples

After two weeks under CO_2 attack, cracked fragments were extracted from the surface layer, which were then covered by a fine conducting layer (metallization process) before undergoing microscopic observation. This coating was necessary to provide the concrete sample with enough electric conductivity for the analysis and it also served to protect the sample from a possible CO_2 reaction with the environment (natural carbonation), which would prevent an

accurate evaluation. Fig.1a illustrates the removal of the sample in sketch form.

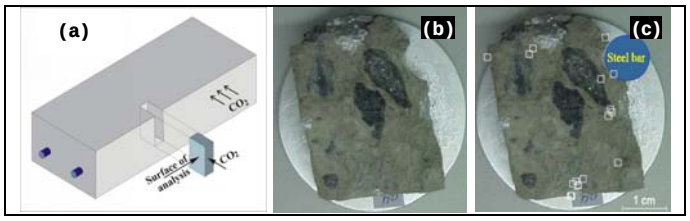

Figure 1 – (a) Sketch showing the removal of test samples; (b) prepared sample for analysis under SEM and (c) sample showing marking of coordinates in the captured images.

During the microscopy analyses, the captured images had their coordinates noted, enabling their marking across the sample's surface (mapping) and thus the verification of their depth inside the covering region (covercrete). Fig.1 (images b and c) clarifies how the marking was made.

In the study of X-ray diffractometry, powdered samples extracted from the covercrete were analyzed at a depth of between 5 mm and 10 mm from the surface. Samples were removed at 120 days of age, that is, before the process of accelerated carbonation, and after two weeks under CO_2 attack. In this manner, alterations in the hydrated paste products due to the CO_2 attack were analyzed.

4 Results and Discussion

4.1 Scanning Electron Microscopy Analysis

The surface of each sample was entirely scanned to identify the characteristics of its topography and the morphology of the compounds originating from cement hydration and carbonation, in the following regions: a) outer region – rim close to the side under study, with carbonation thickness measured by alizarin yellow pH indicator, varying between 5.0 mm and 7.5 mm, depending on the concrete under analysis; b) inner region – non-carbonated region of the covercrete.

The topography of the samples was initially analyzed under low amplifications, comparing the study regions of each concrete. By analyzing each concrete separately, it was noted that generally there was no perceivable difference in density and homogeneity between the regions of the covercrete, except for the concrete with metakaolin. The latter showed in its outer region an aspect of lower density, with irregular cracks throughout that layer, while in the inner region the microstructure proved quite compact visually.

Comparing the different concretes, one notes a greater homogeneity in those with rice-husk ash and silica fume, with a microstructure of relatively high compaction. These two concretes offer, in addition, the highest strengths when cracked for the aspersion of the pH indicators (carbonation study) and the extraction of the samples for SEM. Figs. 2, 3, 4 and 5 illustrate the general aspect of the concrete topographies.

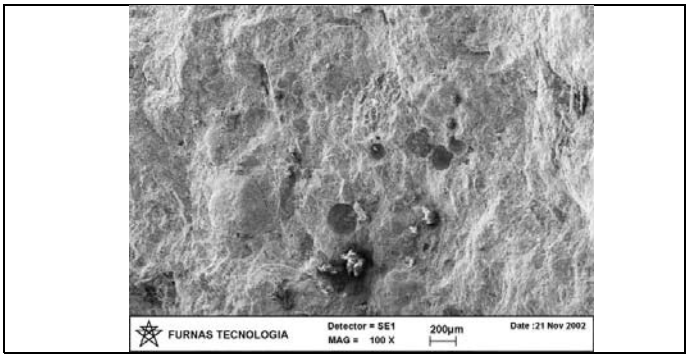

Figure 2 – Reference concrete (without mineral admixture). Image of the inner region.

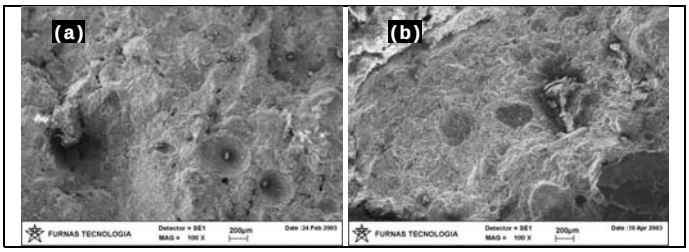

Figure 3 – Concretes with admixtures: (a) fly-ash and (b) blast-furnace slag. Images of the inner region.

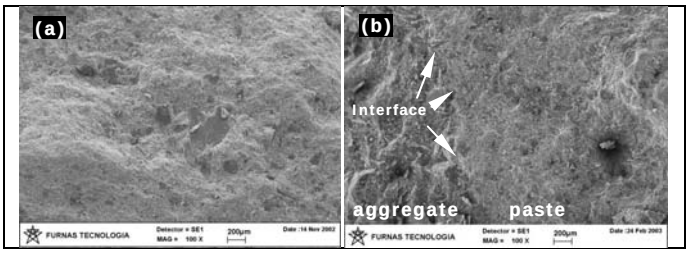

Figure 4 – Concretes with admixtures: (a) rice-husk ash and (b) silica fume. Images of the inner region.

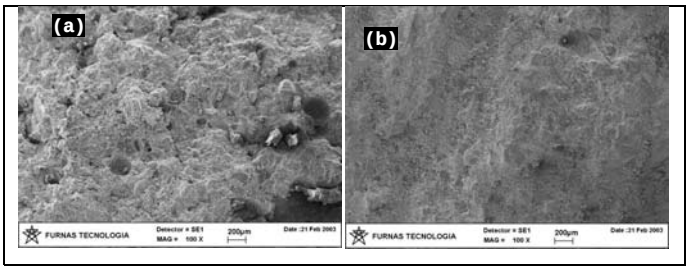

Figure 5 – Concrete with metakaolin admixture: (a) outer region and (b) inner region of covercrete. The density differences in the study regions are quite noticeable.

Generally, it was noted that the reference concretes (Fig.2), fly-ash (Fig.3a) and blast-furnace slag (Fig.3b) yielded a similar microstructural aspect, for the studied contents. Similarities were also noted between the concretes with rice-husk ash (Fig.4a) and silica fume (Fig.4b), which produced structures of greater homogeneity and compactness than the others.

The high compactness of the aggregate-paste interface (transition zone) resulting from the use of mineral admixtures of high specific surface, such as silica fume, is

clearly illustrated by Fig.4b, despite the high w/cm (water-cimentitious materials ratio).

Microstructural alterations, resulting probably from the "wall effect" (of the formworks), were more evident only in the concrete with metakaolin (Fig.5), in which a variation in compactness was noted across the region of covercrete. The outer region (Fig.5a) down to around 5 mm of depth proved less dense, with an aspect closely resembling that of the concretes with fly-ash and blast-furnace slag, while the inner region (Fig.5b) produced visual similarities to those of denser concretes, such as the concrete with rice-husk ash and silica fume.

It was not possible to measure carbonation depth by means of the microscopic analysis of the concrete, but it can be said that the carbonation front proved irregular because t was not always possible to verify the presence of carbonated compounds across the rim that suffered the CO_2 attack. This occurred either because the gas did not spread (perhaps due to the barrier created by an aggregate) or because there was not enough calcium hydroxide (portlandite) in the hydrated paste, thus not enabling an observation of the calcium carbonate crystals ($CaCO_3$ in the form of calcite). However, the carbonated compounds were always noted in some part of the region limited by the pH indicators as being the region of the carbonation front, while in the deeper regions of the covercrete, the non-carbonated region (according to the indicators), such compounds were not present.

The sub-items below discuss the morphological analysis of hydration and carbonation for each of the studied concretes.

4.1.1 Reference Concrete

The reference concrete yielded carbonation products across the outer layer (rims attacked by the carbonic gas), as expected. A great amount of calcite crystals was noted in this region, revealing that this concrete had a greater amount of portlandite before the attack, if compared to the other concretes (with mineral admixtures).

Carbonated compounds of different morphologies were also noted, mainly rhombohedron crystals (approximating cubic and orthorhombic forms) and tetrahedron crystals. Fig.6a illustrates the calcite crystals and it can be noted in Fig.6b that there are overlapping layers of carbonated compounds. Besides the crystals typical of calcite, a carbonated C-S-H structure was found, which resembled dissolved (or meshed) fibers. Fig.7a illustrates the carbonated C-S-H and Fig.7b details the morphology described previously with calcite crystals enveloped by that texture. The microanalysis of that structure revealed that it basically comprised calcium (Ca), silicon (Si), carbon (C) and oxygen (O), while the composition of the calcite crystals resulted in the presence of Ca and O, followed by C and some traces of Si. The spectra for these structures are shown in Fig.8.

As for the non-carbonated region, the presence of portlandite (CH) crystals was verified, both in the pores and scattered across the paste. Contrary to what was expected, the crystals in the latter were always well formed, with hexagonal morphology; however, it must be highlighted that the paste was porous, due to the high w/cm employed, which probably allowed the development of large portlandite crystals. In the non-carbonated region, morphologies typical of C-S-H, with some fibrous structures, were also noted. Fig.9 illustrates the compounds noted in the non-carbonated region.

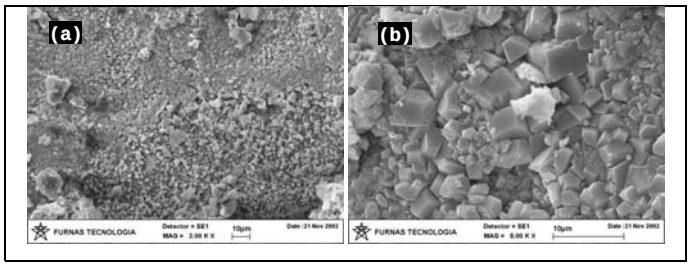

Figure 6 – Reference concrete: (a) presence of calcite crystals of different morphologies and (b) detail of rhombohedron morphology, in which overlapping layers of crystals can be seen.

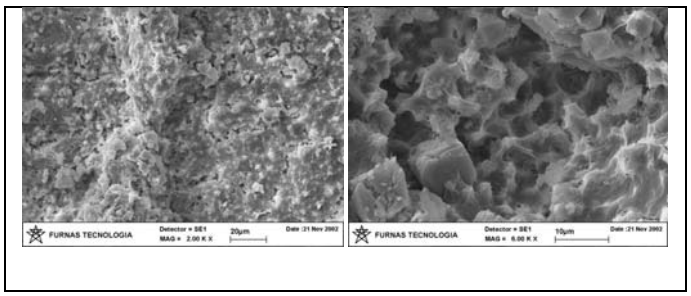

Figure 7 – Reference concrete: (a) carbonated region with surface covered by calcite crystals and carbonated C-S-H and (b) carbonatated C-S-H resembling fibres dissolved or meshed by the CO2 reaction with the calcite crystal.

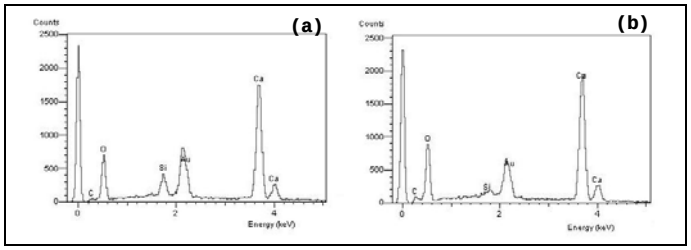

Figure 8 – Reference concrete: (a) spectrum of the carbonated C-S-H structure and (b) spectrum of the calcite structure. The element Au is due to the preparation process.

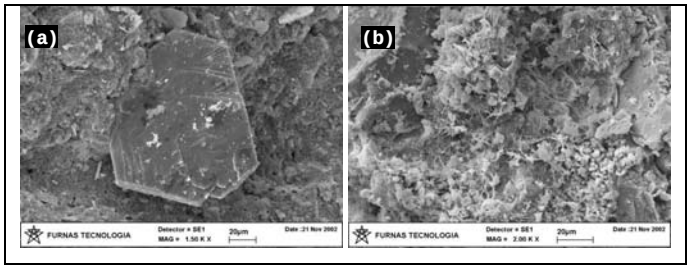

Figure 9 – Reference concrete – non-carbonated region: (a) typical morphology of the CH crystal, scattered across the hydrated paste and (b) products of typical C-S-H morphology.

4.1.2 Concrete with Fly-ash

The concrete with fly-ash admixtures also yielded carbonation products across the outer region, where calcite tetrahedron crystals were noted mainly, as illustrated by Fig.10.

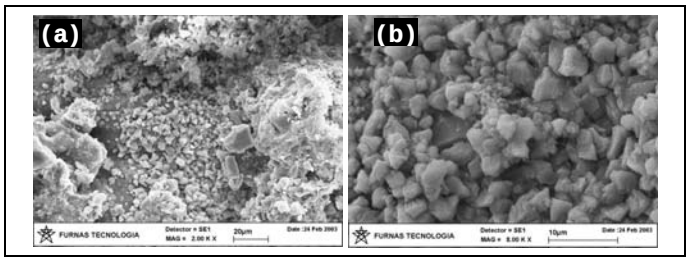

Figure 10 – Concrete with fly-ash: (a) carbonated region with presence of calcity crystals and (b) details of the crystals morphology

In the non-carbonated region compounds typical of C-S-H, similar to those verified in the reference concrete (and shown in Fig.9b), were noted. However, portlandite crystals were not observed, indicating that the pozzolanic reactions may have consumed the large crystals, rendering them unnoticeable in the microstructural analysis.

4.1.3 Concrete with Blast-furnace Slag

In the concrete with blast-furnace slag, calcite crystals were observed, especially in the pores of the outer region, around 5 mm (as illustrated by Fig.11), there being other carbonated compounds, within the carbonated zone.

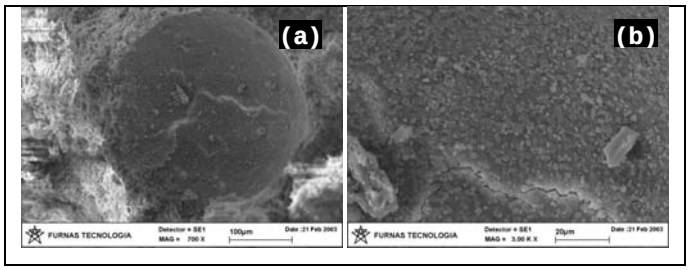

Figure 11 – Concrete with blast-furnace slag: (a) pore in the carbonated region and (b) detail of the calcite crystals impregnated on the pore wall.

Fig.12 illustrates the other carbonated compounds as a possible carbonated hydrated silicate-aluminate of calcium (that is, carbonated C-A-S-H), whose microanalysis yielded Ca, Si, Al (aluminium), Fe (iron), in this order, in addition to traces of carbon, Mg (magnesium) and alkalis (Na and K). Calcite crystals were also noted with traces of other chemical species in their composition. The Fig.13 shows the spectra of the carbonated products.

In the non-carbonated region of this concrete, only void pores or some disaggregated particles of C-S-H were found, there being no evidence of fibrous structures as the ones noted in the reference concretes and with fly-ash.

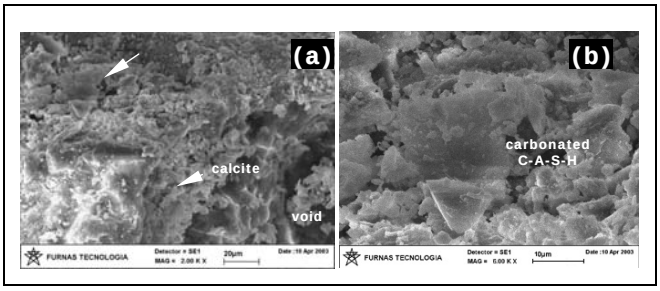

Figure 12 – Concrete with blast-furnace slag: (a) compounds found in the carbonated region and (b) detail of the compound formed by carbonated C-A-S-H.

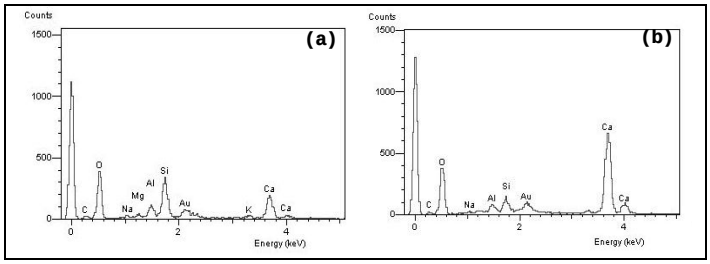

Figure 13 – Concrete with blast-furnace slag: (a) spectrum of the possible carbonated C-A-S-H and (b) spectrum of the calcite crystals compounded with other elements. The element Au is due to the preparation process.

4.1.4 Concrete with Rice-husk Ash

In the carbonated region of the rice-husk ash concrete, compounds typical of calcium carbonate were also verified, as well as products similar to those found in blast-furnace slag, possibly carbonated C-A-S-H. The Fig.14 illustrates the calcite crystals found in the carbonated region of covercrete.

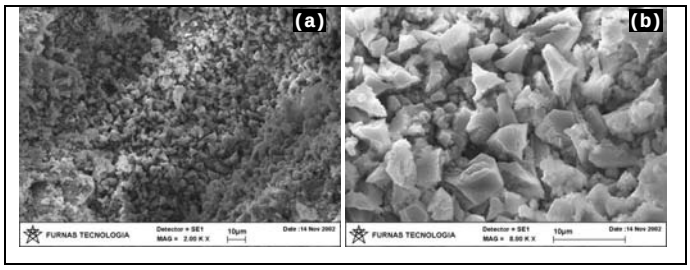

Figure 14 – Concrete with rice-husk ash: (a) carbonated region with the presence of calcite crystals and (b) detail of the tetrahedron morphology of these crystals.

Fig.15a illustrates the other carbonated compound, whose composition under microanalysis basically resulted in Ca, Si, C and Al. Judging by the composition, it is possibly the carbonated silicate-aluminate of calcium.

As for the non-carbonated region, the typical fibrous C-S-H compounds, largely inside some pores, and very few portlandite crystals were noted. The characteristics of this region are illustrated by Fig.15b.

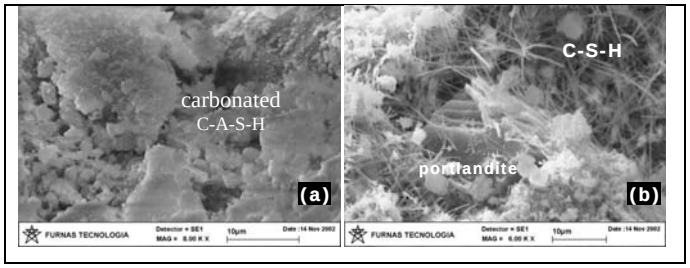

Figure 15 – Concrete with rice-husk ask: (a) carbonated region featuring the compound formed by carbonated C-A-S-H and (b) non-carbonated region highlighting the fibrous material typical of C-S-H and portlandite.

4.1.5 Concrete with Silica Fume

In the carbonated region of the silica fume concrete, the compounds produced in the blast-furnace slag and rice-husk ash, the possible carbonated C-A-S-H and C-S-H, were not found. Only in a few of the pores were calcite crystals found, as illustrated by Fig.16.

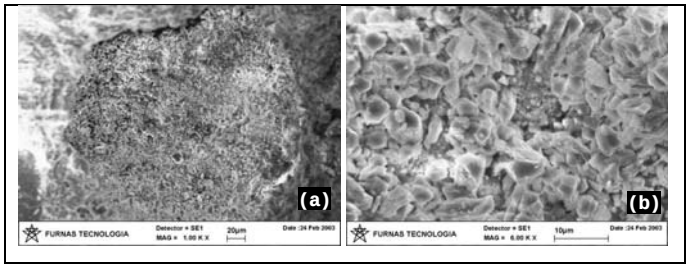

Figure 16 – Concrete with silica fume: (a) pore located in the outer region with carbonated compounds and (b) detail of the calcium carbonate crystals.

As for the non-carbonated region, it featured the same general characteristics of the carbonated zone, that is, an apparently compact C-S-H surface, with void pores, as described in Fig.17a. In the inner region, close to the reinforcement-paste interface, a visually compact structure was noted, but with a higher porosity on the rim of that interface, denoting a possible wall effect resulting from the steel bar. Fig.17b illustratesthat particular aspect.

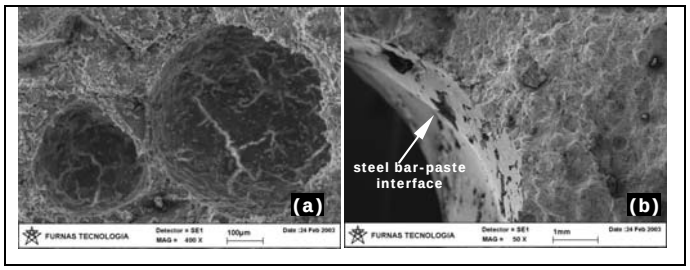

Figure 17 – Concrete with silica fume – non-carbonated region: (a) void pores and (b) reinforcement-paste interface, displaying areas of greater porosity close to the interface circumference, where cracks in the displacement region of the reinforcement are also noted.

4.1.6 Concrete with Metakaolin

In the carbonated region of the metakaolin concrete, no compounds with morphology typical of calcium carbonate were observed, and the pores were void for the most part, with very similar features to those described in the concrete with silica fume.

However, in some points there were findings of products with morphology and composition very similar to those found in the concretes with slag and rice-husk ash, though without carbon in their composition, perhaps because this element is present in lower amounts (not having been detected in the microanalysis) or because they were non-carbonated C-A-S-H and CAH. It is worth noting that these products were found only in the carbonated regions, according to the readings performed by the pH indicator.

The microanalysis of such products basically resulted in Ca, Si and Al, for the irregular particles (Fig.18a) and, in Ca, Si, Al and Fe, for the structures described previously (Fig.18b).

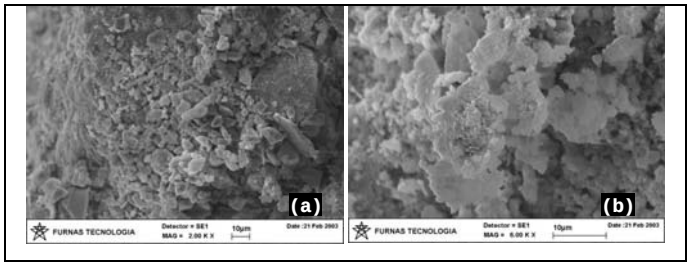

Figure 18 – Concrete with metakaolin: (a) irregular particles verified in the carbonated region and (b) structures similar to those found in the concretes with blast-furnace slag and rice-husk ash.

As for the inner region (non-carbonated), a greater compactness and homogeneity of the microstructure was generally verified, with void pores and C-S-H (or C-A-S-H) across the surface of the region.

4.2 X-Ray Diffractometry Analysis

The diffractograms revealed the compounds resulting from the aggregates, the cement hydration and pozzolanic reactions, as well as from the carbonation process. Some considerations regarding these products are outlined below:

- calcium hydroxide (CH), referred to in the diffractograms as portlandite;
- hydrated calcium silicate, that is, C-S-H(I), C-S-H(II) or tobermorite gel, according to HRB [12], and simply called C-S-H;
- hydrated calcium trisulfoaluminate, that is, ettringite;
- hydrated calcium aluminate, called C_4AH_{13}. According to HRB [12], this compound is indistinguishable from carbonated hydrated calcium aluminate, that is, $C_3A\overline{C}_xH_{12}$, featuring similar crystalline structures whose main interplanar distances are 7,9 Å and 8,2 Å, respectively;
- hydrogarnet, phase structurally related to the mineral garnet ($C_3A_2S_3O_{12}$), in which there is omission of some or all of the silicon, and the possibility of partial or total replacement of the iron by aluminium [7, 17].
- calcium carbonate, constituent of cement portland CPII-F (cement with addition of the carbonatic material) or formed as a result of reaction of CO_2 with calcium hydroxide and other components in concrete. Referred to

in the diffractograms as calcite (main polymorph observed).

Several aspects stand out in these results: firstly, that C-S-H usually appears predominantly amorphous, and is not easily observed by X-ray diffraction, so that it was not detected in all the concretes; secondly, that there can occur an overlapping of the compounds originating from the aggregates with C-S-H, especially of the muscovite compound, in some peaks.

As for calcium carbonate certain aspects stand out. The calcite present in the non-carbonated concretes may originate from the limestone filler that is contained in the portland cement used (CPII F) or from a possible concrete carbonation, occurring naturally up until the test age. Regarding the calcite noted in the carbonated concretes, it originated chiefly by carbonation process in the accelerated test, because by comparing the concrete diffractograms (before and after the CO_2 attack), one can note the decrease or even the disappearance of portlandite peaks and conversely the significant increase in calcite peaks.

The alterations caused by carbonation and referred to in the previous paragraph are easily noted in the X-ray diffractograms, mainly in the peaks that characterize the interplanar distances of portlandite: 2,63 Å, 4,90 Å, and 1,93 Å (determined in the abscissa axes of the diffractograms by the angles 2θ: 34°, 18° and 47°, respectively) and the calcite peaks: 3,04 Å, 2,29 Å, 1,91 Å and 1,87 Å (determined by the angles 2θ: between 29° and 30°, between 39° and 40°, 47° and 49°, respectively). The diffractograms for the concretes (non-carbonated and carbonated) with rice-husk ash, fly-ash, metakaolin, blast-furnace slag, silica fume and reference concrete are shown below (Figs. 19, 20, 21, 22, 23 and 24) with an emphasis on the compounds portlandite and calcite. In a general way, those diffractograms are similar.

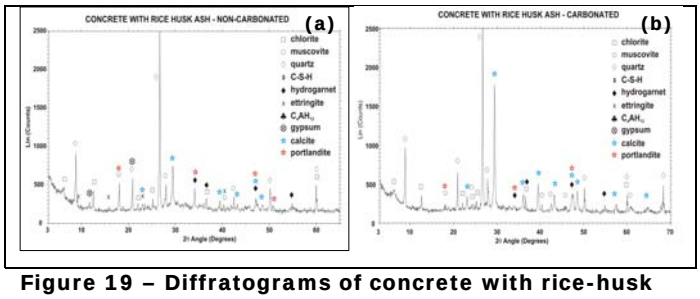

Figure 19 – Diffratograms of concrete with rice-husk ash: (a) before the carbonation process and (b) after the carbonation process.

In the case of concretes with significant aluminium oxide content, namely fly-ash (Fig.20), metakaolin (Fig.21) and blast-furnace slag (whose contents are shown in Table 1), because their hydrated paste is formed essentially by compounds of C-S-H, C-A-S-H or by the hydrated aluminate itself, it was noted that even after carbonation, the compound C_4AH_{13} remained present, which indicates the possibility of it being a carbonated hydrated calcium aluminate, as discussed in the microscopy analysis and mentioned before in this item.

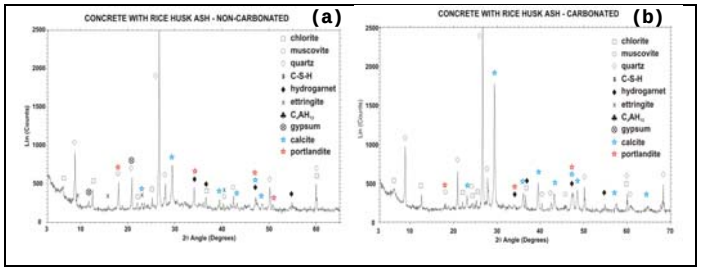

Figure 20 – Diffractograms of concrete with fly-ash: (a) before the carbonation process and (b) after the carbonation process.

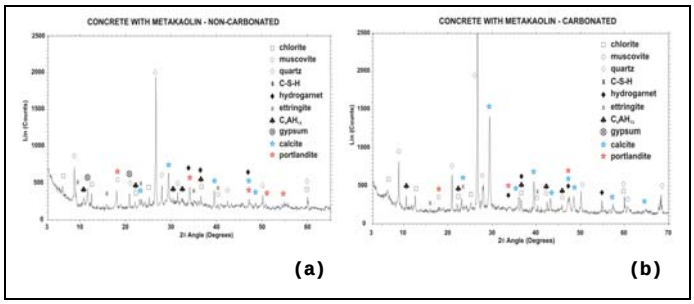

Figure 21 – Diffractograms of concrete with metakaolin: (a) before the carbonation process and (b) after the carbonation process.

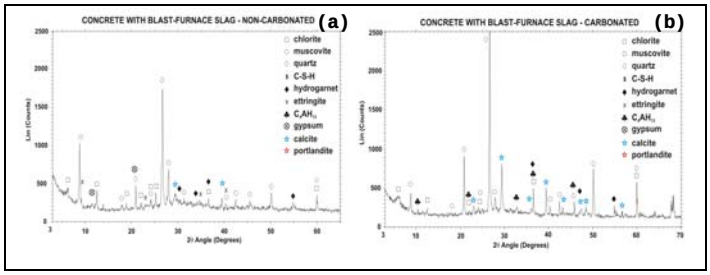

Figure 22 – Diffractograms of concrete with blast-furnace slag: (a) before the carbonation process and (b) after the carbonation process.

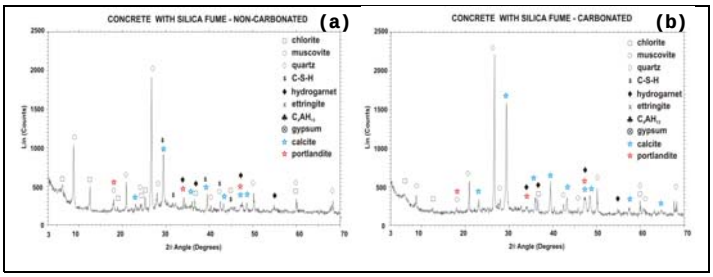

Figure 23 – Diffractograms of concrete with silica fume: (a) before the carbonation process and (b) after the carbonation process.

In particular respect to the concrete with metakaolin (Fig.21), a great amount of calcite was verified, and this material was not clearly seen during microscopy, suggesting that perhaps the irregular particles, exemplified in Fig.18a, could be badly formed calcite crystals.

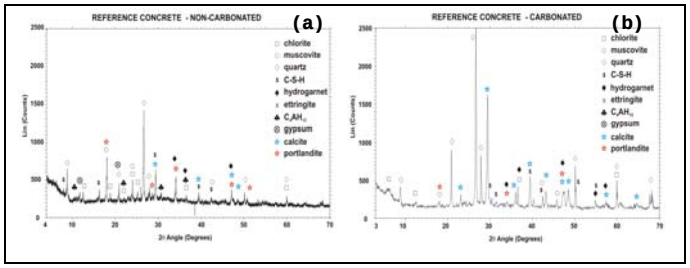

Figure 24 – Diffractograms of reference concrete: (a) before the carbonation process and (b) after the carbonation process.

5 Conclusions

From the microstructural analysis of the concrete, the one performed by scanning electron microscopy served to prove the carbonation of other hydrated paste compounds, with some hydrated calcium silicates and aluminates (C-S-H and C-A-S-H), besides the calcium hydroxide (CH) itself. The X-ray diffractometry analysis, on the other hand, confirmed the development of calcium carbonate (calcite) to the detriment of calcium hydroxide (portlandite) in particular. A greater relative compactness was verified in the microstructure of the concretes with rice-husk ash and silica fume, as had already been observed by Hasparyk et al.[18] in their studies on the microstructure of concretes containing mineral admixtures.

In the present study, a high compactness in the microstructure of the concrete with metakaolin was also noted, but only in the inner region of the covercrete layer. The remaining concretes (reference, fly-ash and blast-furnace slag) produced a visual appearance of compactness which was very similar between them.

The X-ray diffractometry analysis revealed the significant increase in the compound calcite, resulting from the carbonation of the concrete, including in the concretes which, during the SEM observations did not show this compound in a clear manner.

6 Acknowledgements

Our gratitude to FURNAS Centrais Elétricas, in particular the Civil Engineering Technological Center for their technical and financial support afforded in the development of this study. Also to the Coordenação de Aperfeiçoamento de Pessoal de Nível Superior - CAPES, for the financial support in the form of a Master's Program scholarship.

7 References

[1] Aldea, C.M., Young, F., Wang, K. and Shah, S.P., 2000, "Effects of curing conditions on properties of concrete using slag replacement", Cement and Concrete Research, Vol.30, pp.465-472.

[2] Moraes, R.C., Isaia, G.C. and Gastaldini, A.L.G., 2000, "Efeitos da cinza volante, cinza de casca de arroz e filler calcário sobre a resistência mecânica do concreto", In: <http://www.sistrut.com.br/sistrut.html.>

[3] Sabir, B.B., Wild, S. and Bai, J., 2001, "Metakaolin and calcined clays as pozzolans for concrete: review", Cement and Concrete Composites, Vol.23, pp.441-454.

[4] Mehta, P. K. and Monteiro, P. J. M., 1994, Concreto: estrutura, propriedades e materiais, 1st Edition, São Paulo, Pini.

[5] Castro, A., 2003, Influence of mineral additions on the concrete cover durability subject to carbonation. Master's thesis, Federal University of Goiás-Brazil, 217 pp. (download by http://www.gedur.com)

[6] Papadakis, V.G., Vayenas, C.V. and Fardis, M.N., 1991, "Fundamental modelling and experimental investigation of concrete carbonation", ACI Materials Journal, No.88, pp.363-373.

[7] Taylor, H. F. W. ,1997, Cement chemistry, 2nd Edition, London, Thomas Telford.

[8] Nishikawa, T. and Suzuki, K.,1994, "Chemical conversion of C-S-H in concrete", Cement and Concrete Research, Vol.24, pp.176-182.

[9] Kobayashi, K., Suzuki, K. and Uno, Y. , 1994, "Carbonation of concrete structures and decomposition of C-S-H", Cement and Concrete Research, Vol.24, pp.55-61.

[10] Famy, C., Scrivener, K.L. and Crumbie, A.K., 2002, "What causes differences of C-S-H gel grey levels in backscattered electron images?", Cement and Concrete Research, Vol.32, pp.1465-1471.

[11] Matsushita, F., Aono, Y. and Shibata, S., 2004, "Calcium silicate structure and carbonation shrinkage of tobermorite-based material", Cement and Concrete Research, in press.

[12] Highway Research Board, 1972, Guide to compounds of interest in cement and concrete research, Washington, National Academy of Sciences, 53pp.

[13] Alcocel, E.G., Garcés, P. and Chinchón, S., 2000, "General study of alkaline hydrolysis in calcium aluminate cement mortars under a broad range of experimental conditions", Cement and Concrete Research, Vol.30, pp.1689-1699.

[14] Associação Brasileira de Normas Técnicas, 1983, "Agregado para concreto: especificação (NBR 7211)", ABNT, Rio de Janeiro.

[15] Associação Brasileira de Normas Técnicas, 1991, "Cimento Portland composto: especificação (NBR 11578)", ABNT, Rio de Janeiro.

[16] FURNAS, Equipe de Laboratório de Concreto, 1997, Concreto massa, estrutural, projetado e compactado com rolo: ensaios e propriedades. ed. Walton Pacelli de Andrade, São Paulo, Pini.

[17] Oliveira, C. T. A., 2000, Água de poro de pastas de cimento de escória, Tese de Doutorado, Universidade de São Paulo-Brazil, 162 pp.

[18] Hasparyk, N.P., Farias, L.A., Liduário, A.S., Muniz, F.C. and Andrade, M.A.S., 2004, "Study of the behavior of different mineral and pozzolanic admixtures in conventional and roller-compacted concretes with respect to their microstructure and durability", Proceedings of the International Rilem Conference On The Use Of Recycled Materials In Building And Structures, Barcelone, Spain, 2004. 10 pp.